*Engineering Chemistry*
*ISSN: 2813-6535, Vol. 12, pp 25-36*
*doi:10.4028/p-JxUQJ9*

*Submitted: 2025-04-25*
*Revised: 2025-08-20*
*Accepted: 2025-08-27*
*Online: 2025-12-15*

# Characterization and Kinetic Analysis of Activated Flamboyant Tree Pod (*Delonix regia*) Biochar for Crude Oil-Contaminated Water Treatment

Ayodunmomi Esther Olowofoyeku[1,a*], Daniel Gbenga Adekanmi[2,b]

[1]Pan African University Life and Earth Sciences Institute (Including Health and Agriculture), PAULESI, University of Ibadan, Ibadan, Nigeria

[2]Facultad de Ciencias Químicas, Universidad Autónoma de Coahuila, Saltillo, Coahuila, 25280, México

[a*]ayoolowo1122@gmail.com, [b]danieladekanmi@uadec.edu.mx

Corresponding author: ayoolowo1122@gmail.com

**Keywords**: delonix regia, flamboyant tree, activated carbon, adsorption, total petroleum hydrocarbon, remediation.

**Abstract.** Water pollution causes about 1.4 million deaths annually, and in Nigeria, especially in rural areas and the Niger Delta, millions lack access to clean water due to crude oil contamination. This study investigates the use of carbonized Flamboyant (*Delonix regia*) pods as a sustainable, low-cost adsorbent for removing petroleum hydrocarbons from contaminated water, promoting agricultural waste valorization and pollution reduction. Water samples collected from Obiakpor in Port Harcourt, Nigeria, contained 75.22 mg/L of total petroleum hydrocarbons (TPH) and were subsequently used to evaluate the efficiency of the prepared adsorbent. Activated carbon was prepared by washing, drying, carbonizing the pods at 550 °C, chemically activating with KOH, neutralizing, then drying and sieving for uniformity. Carbonization yielded 30.2%, with proximate analysis indicating low moisture (1.86%), moderate ash (4.94%), and high volatile matter (77.81%), which favors thermal stability and pore formation. Scanning Electron Microscopy (SEM) and Brunauer–Emmett–Teller (BET) analysis revealed a highly porous structure with an average pore diameter of 20 μm and a large surface area of 226.4 $m^2/g$. X-ray Diffraction (XRD) confirmed a semi-crystalline structure dominated by graphite (36 wt.%) and silicate minerals, enhancing mechanical strength and π–π interactions. Thermogravimetric Analysis (TGA) showed that thermal stability was maintained between 300–500 °C. Adsorption tests showed TPH removal increased with adsorbent dosage up to 0.2 g, reaching equilibrium afterward. The Freundlich isotherm best described the adsorption ($R^2$ = 0.9104), indicating multilayer adsorption on a heterogeneous surface, supported by high constants ($K_f$ = 166.36; n = 2.35). Kinetic studies indicated rapid adsorption within 25 min, fitting the pseudo-second-order model ($R^2$ = 0.9575). These findings confirm that carbonized Flamboyant tree pods (FTP) are effective, renewable, and thermally stable adsorbents for petroleum-contaminated water treatment.

## Introduction

Water is essential for human survival, but less than 1% of the Earth's total water is available for potable use [1]. Water pollution remains a global crisis, contributing to approximately 1.4 million deaths annually [2, 3]. In Nigeria, where the population exceeds 250 million, nearly 71 million lack access to clean water, and this is further complicated by the inadequate access to basic sanitation facilities by over 130 million [4]. The water problem is usually more critical in rural areas, exposing millions to significant health risks [5]. The inhabitants of the Niger Delta region of Nigeria face acute water pollution challenges due to oil spills, industrial discharge, and poor waste management, which threaten health and livelihood [6]. Since the discovery of crude oil in the 1950s, weak environmental regulations have exacerbated ecological degradation, especially in this region [7]. Ensuring access to clean water is a fundamental human right, and this makes water quality control a necessary global priority [8]. Conventional remediation techniques such as chemical precipitation, reverse osmosis, and ion exchange are widely employed but present challenges, including high operational costs and

significant sludge generation. Hence, the search for cost-effective and environmentally sustainable alternatives is imperative [9].

Agricultural waste, such as husks, cobs, and pods of plants, is a viable source of biomass that can be converted into low-cost, sustainable remediation tools, reducing cleanup costs and aligning with circular economy principles through waste valorization [10]. Carbonized biomass sorbents are characterized by high oil sorption capacities of up to 10.1 g/g through micro/mesoporous structures and large surface areas (>2000 $m^2/g$) [11]. Their properties are further optimized through methods such as KOH activation to enhance hydrophobicity and improve selective oil-water separation. Since they are derived from various biomass sources [12]. Their reusability (via solvent/thermal regeneration) and post-use applications as biochar for soil conditioning or carbon storage further minimize waste and long-term environmental impact [13]. Floating variants (e.g., carbonized sphagnum moss) enable easy recovery, while their biodegradability eliminates microplastic risks, ensuring ecological safety compared to synthetic alternatives. This synergy of performance, scalability, and sustainability positions carbonized biomass as a frontline solution for oil spill remediation [14, 15].

Flamboyant tree (*Delonix regia*), a member of the *Fabaceae* family, is often viewed as agricultural waste but has shown significant potential in various applications. Adeniyi et al. utilized *Delonix regia* stem waste to produce biochar through carbonization at 500 °C, resulting in a material with a surface area of 356 $m^2/g$, mesoporosity, and functional groups (OH, C=O), suitable for soil amendment and water purification [16]. Also, Emenike et al. demonstrated the effectiveness of *Delonix regia* pod-derived biochar in removing phenol from wastewater, achieving an 82.3% removal efficiency under optimal conditions (60 °C, 60 min) through a non-spontaneous and irreversible process that fits the Freundlich isotherm and pseudo-second-order kinetic models [17]. In another study, Azeez et al. explored the adsorption of Rhodamine B dye onto activated carbon derived from *Delonix regia* seeds and pods, achieving high removal efficiencies of 99.16% and 98.36%, with the process best described by the Freundlich isotherm and pseudo-second-order kinetics [18]. These studies collectively highlight the versatility and potential of Flamboyant tree parts in environmental remediation and renewable energy applications.

Building on previous studies that have demonstrated the effectiveness of Flamboyant tree parts in removing various contaminants, Azeez et al. [18], Emenike et al. [17], Ibrahim et al. [19], and Latinwo et al. [20] his research investigates the biosorption capacity, characterization, and kinetic behavior of activated carbon derived from Flamboyant pods for the removal of total petroleum hydrocarbons (TPH) from crude oil-contaminated water in Obiakpor Local Government Area, Port Harcourt, Rivers State, Nigeria. In this study, a simple and low-cost adsorbent was prepared from Flamboyant pods, thoroughly characterized, and its adsorption properties and kinetics were investigated by varying dosage and contact time. The objective was to evaluate the adsorbent's effectiveness for the environmental remediation of petroleum-contaminated water.

## Materials and Methodology

### Water Sampling and Collection of FTP

Water samples were collected from the three most frequently used drinking water sources in each selected community within Obiakpor Local Government Area, following community consent and guidance. Samples were collected in pre-cleaned, clearly labeled glass bottles to prevent contamination and immediately stored at 4 °C during transport to the laboratory. Analysis was conducted within 24 h to minimize degradation and maintain sample integrity. All sampling equipment and containers were handled using disposable gloves and standard quality assurance protocols, including the use of field blanks and proper documentation [21]. The average Total Petroleum Hydrocarbon (TPH) concentration in the water sources was determined using standard analytical procedures [22], yielding a baseline value of 75 ± 0.15 mg/L. This concentration was used for subsequent adsorption studies.

### Preparation, Carbonization and Activation of the Adsorbent

The preparation of activated carbon from *Delonix regia* pods followed a multi-step process similar to that described by Emenike et al. [17]. Initially, the pods were thoroughly washed with deionized water, soaked, and rinsed before being sun-dried for five days. They were then oven-dried at 80 °C for 20 h until a constant weight was achieved. The dried material was crushed and sieved using a 250 µm mesh filter. Subsequently, the powdered material underwent carbonization in a muffle furnace, heated at a rate of 2 °C/min to 550 °C, and maintained for 2 h. Following carbonization, the material was activated using 0.1 M KOH at a 1:2 ratio (carbonized material : KOH) at 130 °C for 4 h with periodic stirring. The activated adsorbent was then washed with HCl and deionized water until pH = 7. Finally, the material was dried in an electric oven, sieved for uniformity, and stored in an airtight container for further characterization.

### Adsorbent Characterization

The characterization of the activated FTP adsorbent was conducted using a comprehensive suite of analytical techniques to assess its properties. Proximate analysis, following ASTM D3172-13, was performed to determine the moisture content, ash content, volatile matter, and fixed carbon [23]. Additionally, iodine number analysis (ASTM D4607-14) was used to evaluate microporosity and adsorption capacity [24]. The bulk density of the adsorbent was measured using the tap density method to assess packing efficiency [25]. The surface morphology was determined using Scanning Electron Microscopy (SEM, JEOL JSM-IT300, JEOL Ltd., Japan). Meanwhile, surface area and pore size distribution were determined through Brunauer–Emmett–Teller (BET) analysis (Micromeritics ASAP 2020, Micromeritics Instrument Corp., USA). X-ray Diffraction (XRD) analysis, using an Empyrean X-ray Diffractometer (Malvern Panalytical, Netherlands), was conducted to identify the present phases. Thermogravimetric Analysis (TGA) and Differential Thermal Analysis (DTA) were performed using a PerkinElmer STA 6000 thermal analyzer (PerkinElmer Inc., USA) to evaluate thermal stability, decomposition behavior, and weight loss under increasing temperatures [26, 27].

### Adsorption Efficiency and Kinetics Studies

Adsorption studies were conducted using the modified method of Latinwo et al. [20] after preliminary experiments to evaluate the efficiency of the adsorbent in removing Total Petroleum Hydrocarbons (TPH) from contaminated water. The experimental conditions, that is, adsorbent dosage and contact time, were varied to determine optimal adsorption parameters.

### Effect of Adsorbent Dosage

To study the effect of adsorbent dosage on total petroleum hydrocarbon (TPH) removal, batch adsorption experiments were conducted using carbonized FTP powder treated with potassium hydroxide (KOH). The pod powder was sieved to a particle size of less than 250 µm before use. The adsorbent mass was varied from 0.05 to 0.25 g and added to 50 mL of TPH-contaminated water placed in 100 mL conical flasks. The initial TPH concentration was kept constant at 75.22 mg/L across all samples. The flasks were agitated using a digital orbital shaker at a fixed speed of 130 rpm for a contact time of 21 min at room temperature (25 ± 2 °C). After the set mixing period, the mixtures were filtered to remove the solid adsorbent. The clear filtrates were analyzed using UV-Vis spectrophotometry at 272 nm to determine the remaining TPH concentration. Removal efficiency (%) was calculated using:

$$\text{Removal Efficiency} = ((C_i - C_f) / C_i) \times 100 \quad (1)$$

Where $C_i$ is the initial TPH concentration (mg/L) and $C_f$ is the final TPH concentration (mg/L). All experiments were performed in triplicate, and average values with standard deviations were reported.

### Adsorption Isotherm Studies

To study the adsorption isotherms of Total Petroleum Hydrocarbons (TPH) on the carbonized *Delonix regia* pod (FTP) adsorbent, batch experiments were conducted by varying the initial TPH concentrations while keeping all other parameters constant. A fixed adsorbent dose of 0.1 g was added

to 50 mL of TPH-contaminated water with different initial concentrations (ranging from 25 to 125 mg/L). The flasks were agitated at 130 rpm and room temperature (25 ± 2 °C) for 25 min, based on the equilibrium time determined from preliminary kinetics studies. After equilibration, the mixtures were filtered, and the remaining TPH concentrations were measured using UV-Vis spectrophotometry at 272 nm.

Two adsorption isotherm models were applied:

Freundlich Isotherm:

$$\log q_e = \log K_f + \frac{1}{n}\log C_e \quad (2)$$

Langmuir Isotherm

$$\frac{C_e}{q_e} = \frac{1}{Q_{max}K_L} + \frac{C_e}{Q_{max}} \quad (3)$$

where $q_e$ = amount of TPH adsorbed per gram of adsorbent at equilibrium (mg/g)
$C_e$ = equilibrium concentration of TPH in solution (mg/L)
$K_f$ = Freundlich constant (adsorption capacity)
n = adsorption intensity
$Q_{max}$ = maximum monolayer adsorption capacity (mg/g)
$K_L$ = Langmuir constant related to binding affinity (L/mg)

**Adsorption Kinetics Studies**

Kinetics experiments were conducted using a fixed TPH concentration of 75.22 mg/L and 0.1 g of the carbonized FTP adsorbent in 50 mL of solution. Samples were withdrawn at 5, 10, 15, 20, 25, 30, and 35 min, filtered, and analyzed for TPH concentration. Removal efficiency was calculated using Equation (1). Kinetic data were fitted to the following models:

Pseudo-First-Order Model:

$$\log(q_e - q_t) = \log q_e - \frac{k_1}{2.303}t \quad (4)$$

Pseudo-Second-Order Model:

$$\frac{t}{q_t} = \frac{1}{k_2 q_e^2}q_e + \frac{t}{q_e} \quad (5)$$

Intraparticle Diffusion Model**:**

$$q_e = k_{id}t^{0.5} + C \quad (6)$$

where:
$q_t$ = adsorption at time t (mg/g)
$q_e$ = equilibrium adsorption (mg/g)
$k_1$ = pseudo-first-order rate constant ($min^{-1}$)
$k_2$ = pseudo-second-order rate constant (g/mg·min)
$k_{id}$ = intraparticle diffusion rate constant ($mg/g \cdot min^{0.5}$)
$C$ = intercept related to boundary layer thickness
The slope and intercepts of the linearized plots were used to calculate the kinetic constants, and model fit was assessed by the $R^2$ values.

**Statistical Analysis**

All experiments were performed in triplicate, and average values were reported. Standard deviations were calculated to assess variability. Control experiments without adsorbent were conducted to account for natural degradation effects.

## Results and Discussion

### Physicochemical Characterization of FTPs

The carbonized FTP adsorbent in this study achieved a yield of 30.2%, surpassing the values reported for the plant's stem by Adeniyi et al. (26.57%) and Vargas et al. (27.8%), while nearing the higher yield of 41.09% documented by Sugumaran et al. [28]. Tables 1 and 2 present the proximate and physicochemical properties of the material, highlighting its adsorption suitability. The low moisture content (1.86%) enhances thermal stability and minimizes water interference during adsorption, while the moderate ash content (4.94%) and high volatile matter (77.81%) indicate strong reactivity during carbonization, facilitating pore formation and structural development essential for adsorption [29, 30]. The fixed carbon content of 15.39% aligns with values reported by Alonge et al. [31] (19.11%) and Sugumaran et al. [28] (5.20%), while other parameters are consistent with findings from similar studies. The bulk density of 0.63 g/mL supports practical adsorption applications and matches the 0.52 g/mL reported by Latinwo et al. [32], while the iodine value of 1468.65 mg $I_2$/g reflects a high surface area, indicating strong adsorption capacity consistent with Sugumaran et al.'s results.

**Table 1.** Proximate Analysis of Carbonized FTP.

| Parameter | Value (%) |
|---|---|
| Moisture Content | 1.86 |
| Ash Content | 4.94 |
| Volatile Matter | 77.81 |
| Fixed Carbon | 15.39 |

**Table 2.** Physicochemical Properties of the Carbonized Pod.

| Parameter | Value |
|---|---|
| Yield | 30.2% |
| Bulk Density | 0.63 g/mL |
| Iodine Number | 1468.65 mg $I_2$/g |

### Characterization of the Carbonized Pods

### Morphology, Surface Roughness and Porosity

The SEM analysis of carbonized FTP adsorbent revealed irregularly shaped particles up to 100 μm in size, with pores averaging 20 μm in size and hive-like hierarchical cells indicative of mesopores and macropores, which enhance hydrocarbon capture and adsorption potential (Fig. 1). Azeez et al. [18], Sugumaran et al. [28], and Ibrahim et al. [19] reported a similar porous structure with a more sheet-like appearance. The surface roughness measurements showed a root mean square (RMS) roughness of 70.74 μm and a mean roughness of 60.24 μm, confirming a rugged morphology that complements the porosity observed in BET analysis. Negative skewness (Ssk = –0.358) and kurtosis (–0.9996) indicate a valley-rich surface, providing entrapment zones for contaminants, while the high surface area of 27,422.4 $\mu m^2$ and slope of $1.17 \times 10^3$ further supported enhanced molecular interactions during adsorption. BET analysis measured a surface area of 226.399 $m^2$/g, with nitrogen adsorption at 77.350 K showing a strong correlation (r = 0.9973) in the linear BET region, validating the reliability of the data. A BET C constant of 3.457 suggested moderate adsorbate–adsorbent interactions favoring physisorption, desirable for reversible adsorption processes. Degassing at 250 °C for 3 h ensured contaminant-free pores, enhancing accessibility for hydrophobic organic pollutants like TPH. Together, these results demonstrate that the carbonized FTP adsorbent possesses a mesoporous structure with high adsorption capacity, making it suitable for environmental remediation applications.

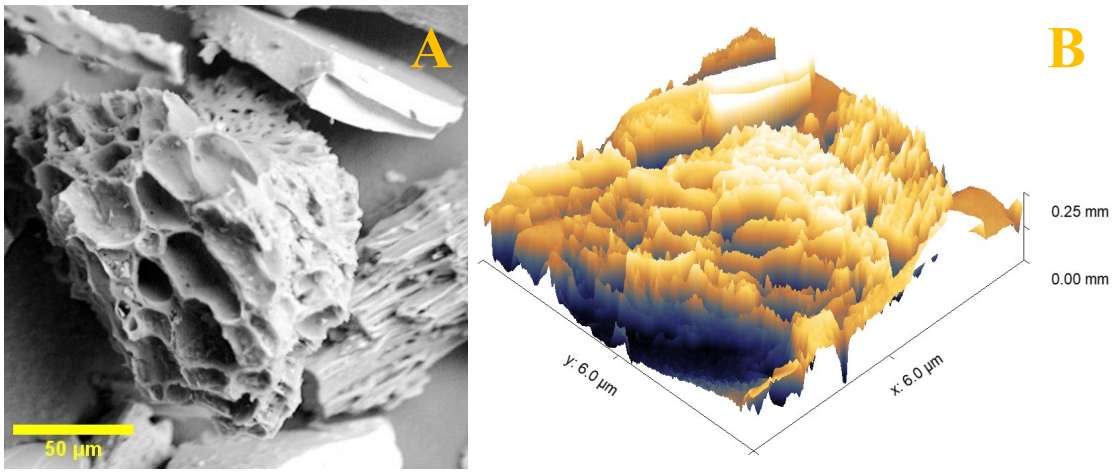


**Fig. 1.** SEM and surface roughness image of carbonized FTP adsorbent.

**Table 3.** Surface roughness of the carbonized FTP adsorbent.

| Parameter | Value | Implication |
|---|---|---|
| RMS Roughness (Sq) | 70.74 µm | High surface variation |
| Mean Roughness (Sa) | 60.24 µm | Reflects surface irregularity |
| Skewness (Ssk) | –0.358 | Valley-dominated topography |
| Kurtosis (Sku) | –0.9996 | Flattened surface peaks |
| Max Peak Height (Sp) | 111.87 µm | Highest elevation from the average line |
| Max Pit Depth (Sv) | 143.13 µm | Deepest depression from the average line |
| Surface Area | 27,422.4 $\mu m^2$ | Large interaction area |
| Surface Slope (Sdq) | $1.17 \times 10^3$ | Indicates steep topographic change |

**Table 4.** BET Parameters of carbonized FTP adsorbent.

| Parameter | Value | Unit |
|---|---|---|
| BET Surface Area | 226.399 | $m^2/g$ |
| Pore Diameter (mode) | 2.94 | nm |
| DA Micropore Volume | 0.205 | $cm^3/g$ |
| BET C Constant | 3.457 | — |
| Correlation Coefficient | 0.997 | — |
| Degassing Temperature | 250 | °C |
| Degassing Time | 3.0 | h |
| Adsorption Temperature | 77.35 | K |
| DA Best E | 0.701 | kJ/mol |

**XRD Analysis**

The XRD analysis of carbonized FTP, presented in Fig. 2, shows a semi-crystalline structure, primarily composed of graphite (36 ± 13 wt%), which enhances π–π interactions and supports the efficient adsorption of hydrophobic TPH molecules. Silicon oxide (27 ± 7 wt%) and Dinite (29 ± 8 wt%) are the main silicate phases, contributing to the material's structural rigidity and thermal stability. The presence of Osumilite (5 ± 4 wt%) and Marialite (2 ± 3 wt%) suggests mineral retention or ash formation during carbonization, potentially adding polar sites for contaminant anchoring. Specifically, the XRD pattern had a broad peak near $2\theta = 24.5°$, which is associated with amorphous carbon (C (002)), and smaller peaks at around $2\theta = 43°$ traceable to disordered carbon [33, 34]. The presence of minerals like silicon oxide, along with carbon, is common in biomass-based materials and has been reported in previous studies [34, 35]. Their combination with amorphous carbon creates a mixed structure with tiny crystalline areas, which allows different interaction mechanisms during adsorption. This mineral-rich, semi-crystalline biochar offers good structural strength, porosity, and

surface variety, making it useful for environmental cleanup, especially in removing total petroleum hydrocarbons (TPH).

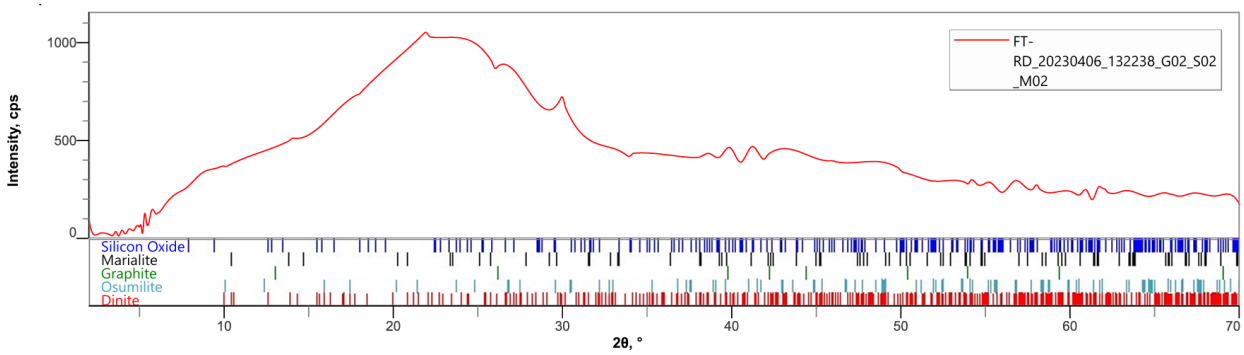


**Fig. 2.** XRD pattern of carbonized FTP adsorbent.

## TGA-DTA Analysis

The TGA-DTG result of the carbonized FTP sample (Fig. 3) was similar to that observed by Adeniyi et al. The result revealed a significant weight loss of about 90% between 300 °C and 500 °C, primarily due to the decomposition of volatile matter and organic components. The peak weight loss rate occurs at approximately 430 °C, marking the main thermal degradation zone, which reflects the high content of pyrolyzable organic compounds. This decomposition pattern aligns with the thermal behavior of biomass components: hemicellulose decomposes between 260 – 330 °C, cellulose between 310 – 464 °C, and lignin over a broader range up to 950 °C due to its complex aromatic structure [36]. Beyond 550 °C, minimal weight change indicates the presence of stable carbonaceous residues and inorganic minerals, consistent with the graphite and silicate phases detected by XRD. The initial weight loss below 150 °C is negligible, confirming the low moisture content, and the biochar exhibits higher thermal stability than raw biomass, with a peak degradation temperature of 390 °C.

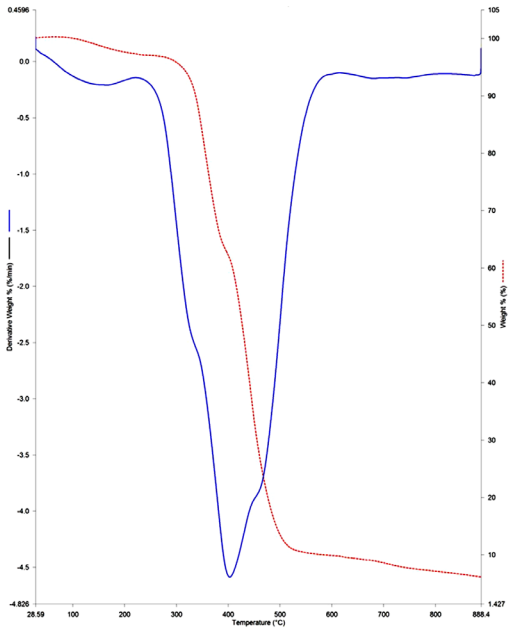


**Fig. 3.** TGA-DTA curves of carbonized FTP adsorbent.

## Adsorption and Kinetic Properties

### Effect of Adsorbent Dosage on TPH Removal and Adsorption Isotherms of TPH on Carbonized Pod

As stated earlier, the initial TPH concentration in the contaminated water samples used for adsorption studies was 75.22 mg/L, as determined in earlier studies [37]. The results in Table 5 show that increasing the adsorbent dosage improves the removal efficiency of total petroleum hydrocarbons

(TPH) by providing more active sites for adsorption [26, 27]. However, beyond 0.2 g, the efficiency gains become minimal, indicating that the system is nearing saturation or equilibrium, as most TPH molecules have already been adsorbed and additional adsorbent contributes little to further removal. At this stage, adding more adsorbent does not significantly enhance removal because there are not enough TPH molecules left to occupy the extra sites. This trend aligns with findings from previous studies, confirming a limit to the benefits of increasing adsorbent dosage [26].

**Table 5.** TPH removal efficiency at varying adsorbent dosages.

| Dosage (g) | Initial TPH (mg/L) | Final TPH (mg/L) | Removal Efficiency (%) |
|---|---|---|---|
| 0.05 | 75.22 ± 0.15 | 32.85 ± 1.2 | 56.33 ± 1.6 |
| 0.10 | 75.22 ± 0.15 | 21.40 ± 1.0 | 71.55 ± 1.3 |
| 0.15 | 75.22 ± 0.15 | 11.65 ± 0.8 | 84.52 ± 1.1 |
| 0.20 | 75.22 ± 0.15 | 4.51 ± 0.5 | 94.01 ± 0.7 |
| 0.25 | 75.22 ± 0.15 | 3.85 ± 0.4 | 94.88 ± 0.5 |

The adsorption of Total Petroleum Hydrocarbons (TPH) using carbonized FTP was best described by the Freundlich isotherm model as presented in Fig. 4. The Freundlich plot gave a straight line with a high $R^2$ value of 0.9104, showing a strong fit according to equation (2). From the slope and intercept of the plot, the values of $K_f$ and n were calculated as 166.36 and 2.35, respectively. Since $1 < n < 10$, the adsorption is considered favorable. The high $K_f$ value also indicates a high adsorption capacity. This model suggests that the adsorbent surface is uneven and supports multilayer adsorption (equation 3). The plot gave an $R^2$ value of 0.8385, which was lower than that of the Freundlich model. The slope and intercept gave a maximum adsorption capacity $Q_{max}$ of 1025.81 mg/g and a Langmuir constant $K_L$ of 0.0825 L/mg. This result implies some level of monolayer adsorption on the surface, but the lower $R^2$ value shows that the surface is not completely uniform. Overall, the Freundlich model fits the experimental data better, confirming that adsorption occurs on a heterogeneous surface with more than one type of binding site. TPH adsorption using carbonized FTPs follows the Freundlich model better than the Langmuir model, indicating an uneven surface that supports multilayer adsorption. High values of $K_f$ and n confirm a strong attraction between the adsorbent and TPH [38, 39].

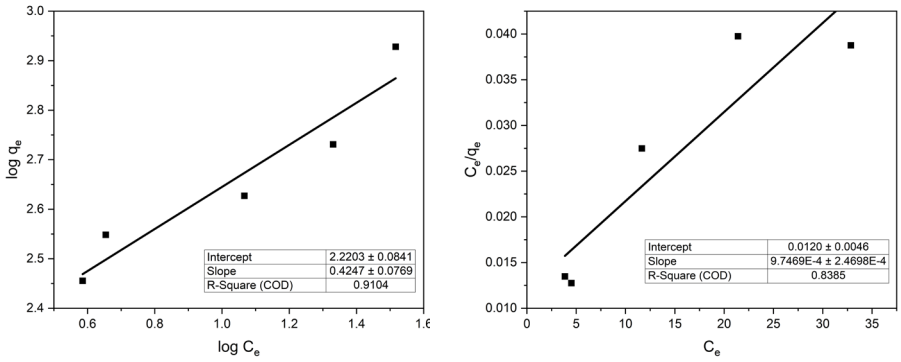


**Fig. 4.** Adsorption isotherms of the carbonized FTPs; Freundlich plot (left) and Langmuir plot (Right).

**Effect of Contact Time on TPH Removal and Adsorption Kinetics of the Carbonized Pods**

Contact time also affected removal efficiency, as reported by other studies (Table 6**)**, suggesting a time-dependent diffusion of TPH molecules onto the adsorbent surface. The sharp rise in efficiency up to 25 min indicates rapid adsorption due to the high availability of active sites. Beyond this point, the rate of increase slowed, implying that adsorption sites were becoming saturated, and the system was approaching equilibrium.

**Table 6.** TPH Removal Efficiency at Varying Contact Times.

| Contact Time (min) | Initial TPH (mg/L) | Final TPH (mg/L) | Removal Efficiency (%) |
|---|---|---|---|
| 5 | 75.22 ± 0.15 | 67.21 ± 0.31 | 10.65 ± 1.5 |
| 10 | 75.22 ± 0.15 | 53.56 ± 0.21 | 28.85 ± 1.0 |
| 15 | 75.22 ± 0.15 | 39.48 ± 0.26 | 47.61 ± 1.2 |
| 20 | 75.22 ± 0.15 | 28.64 ± 0.11 | 61.89 ± 0.7 |
| 25 | 75.22 ± 0.15 | 23.12 ± 0.15 | 69.30 ± 0.9 |
| 30 | 75.22 ± 0.15 | 18.24 ± 0.11 | 75.74 ± 0.7 |
| 35 | 75.22 ± 0.15 | 15.62 ± 0.13 | 79.32 ± 0.9 |

TPH adsorption efficiency onto carbonized FTPs increased rapidly within the first 25 min, then slowed significantly to reach 79.32% at 35 min. This pattern suggests that the system was approaching equilibrium, as also observed by Ji et al. [26] and Esmaeili and Saremnia [40], and that most active sites were occupied early in the process. To further understand this behavior, the kinetics of adsorption were analyzed using three models: pseudo-first-order, pseudo-second-order, and intraparticle diffusion (Fig. 5). The pseudo-first-order model showed a poor fit ($R^2$ = 0.0185), indicating that physical adsorption was not the dominant mechanism. Conversely, the pseudo-second-order model yielded a high $R^2$ value of 0.9575, along with a slope of 0.5740 and an intercept of -1.3413, pointing to chemisorption involving electron sharing or exchange between TPH and the adsorbent. The intraparticle diffusion model, with an $R^2$ of 0.0000, confirmed that pore diffusion was not the rate-limiting step. Thus, the pseudo-second-order model provides the most accurate representation of the adsorption mechanism under the studied conditions. The analysis suggests that the adsorption of TPH onto KOH-treated carbonized FTPs is best described by chemisorption, supported by the high fit of the pseudo-second-order model and the poor fit of the pseudo-first-order model. The negligible effect of intraparticle diffusion further supports this conclusion, highlighting that chemical interactions dominate over physical adsorption or pore diffusion. KOH activation introduces oxygen-containing functional groups such as carboxyl and hydroxyl groups, which enhance surface reactivity and promote strong chemical bonding with TPH molecules. This leads to the formation of covalent bonds, ion exchange, and π-π interactions, which increase the adsorption capacity and specificity [41].

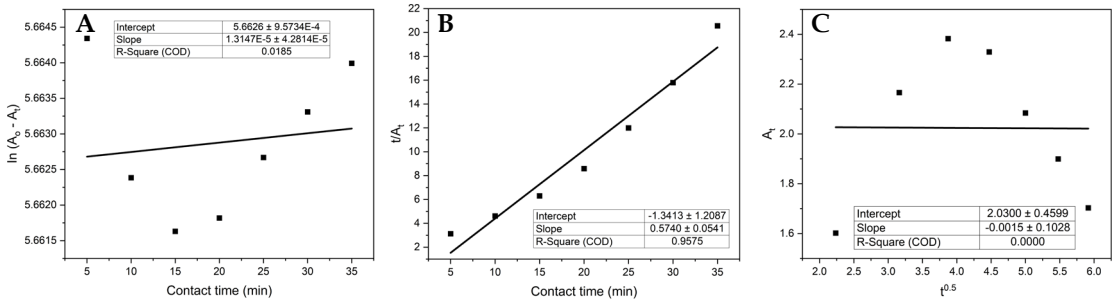


**Fig. 5.** Adsorption kinetics plot of the carbonized FTPs: Pseudo-first-order model (A), Pseudo-second-order model (B), and intraparticle diffusion model (C).

These findings align with similar studies on KOH-activated biochar, which also report chemisorption as the primary mechanism for TPH adsorption. Previous research on Flamboyant and other carbon-based adsorbents further supports the observation that pseudo-second-order kinetics are indicative of chemisorption [38, 39, 41]. For example, Ji et al. [26] used a corn stalk biochar (SBC) composite modified with nano zero-valent iron was used, achieving up to 75% removal efficiency. The process followed the Freundlich isotherm and pseudo-second-order kinetics. Similarly, Nazal et al. [42] used seagrass biochar to remove 98.8% of TPH, fitting both Langmuir and Freundlich isotherms, and demonstrating strong adsorption performance.

## Conclusion

The carbonized flamboyant tree pod (FTP) developed in this study shows strong potential as a sustainable, low-cost adsorbent for removing total petroleum hydrocarbons (TPH). The carbon yield of 30.2% surpasses many similar biomasses. Favorable proximate properties such as low moisture (1.86%), moderate ash (4.94%), and high volatile matter (77.81%) support energy efficiency and effective pore development. The high iodine number (1468.65 mg $I_2$/g) indicates a well-developed surface area. SEM and surface roughness analyses showed a rugged, porous structure with an average pore diameter of 20 μm and a BET surface area of 226.399 $m^2$/g, enhancing molecular trapping. Mesopores and macropores, along with the moderate BET C constant (3.457), support physisorption and reversible adsorption. XRD confirmed a semi-crystalline structure comprising graphite (36 wt%) and silicate phases, which enables strong π–π interactions and mechanical strength. Thermogravimetric analysis revealed high thermal resistance, with a major weight loss occurring at 300–500 °C due to biomass decomposition, confirming the structural integrity under heat. TPH adsorption increased with dosage up to 0.2 g before equilibrium. Freundlich isotherm ($R^2$ = 0.9104; $K_f$ = 166.36; n = 2.35) fit best, indicating multilayer adsorption on a heterogeneous surface, though Langmuir also applied ($R^2$ = 0.8385). Kinetic data aligned with the pseudo-second-order model ($R^2$ = 0.9575), confirming chemisorption. These findings demonstrate that carbonized FTP is an efficient, thermally stable, and renewable adsorbent with excellent structural features, making it suitable for the large-scale remediation of petroleum-contaminated water and soil.

## References

[1] R.K. Mishra, Fresh Water availability and Its Global challenge, Brit. J. Multi. Adv. Stud. 4 (2023) 1-78.

[2] E.J. Isukuru, J.O. Opha, O.W. Isaiah, B. Orovwighose, and S.S. Emmanuel, Nigeria's water crisis: Abundant water, polluted reality, Cleaner Water 2 (2024) 1-33.

[3] L. Lin, H. Yang, and X. Xu, Effects of Water Pollution on Human Health and Disease Heterogeneity: A Review, Front. Environ. Sci. 10 (2022) 1-16.

[4] B. Shehu, and F. Nazim, "Clean Water and Sanitation for All: Study on SDGs 6.1 and 6.2 Targets with State Policies and Interventions in Nigeria," *Environ. Sci. Proc.,* 15, 2022].

[5] S. Singh, Chapter 3 - Water pollution in rural areas: Primary sources and associated health issues: S. Madhav, A.L. Srivastav, S. Chibueze Izah and E.v. Hullebusch, eds., Water Resources Management for Rural Development, Elsevier, 2024, pp. 29-44.

[6] D.R.E. Ewim, O.F. Orikpete, T.O. Scott, C.N. Onyebuchi, A.O. Onukogu, C.G. Uzougbo, and C. Onunka, Survey of wastewater issues due to oil spills and pollution in the Niger Delta area of Nigeria: a secondary data analysis, Bull. Natl. Res. Cent. 47 (2023) 1-20.

[7] O.C. Chidiobi, and J.C. Ibekwe, Oil Exploitation, Environmental issues and resource curse in a post-colonial Niger Delta Region of Nigeria: the unending search for peace, 1960–2009, ASSRJ 9 (2022) 373-394.

[8] M. Fida, P. Li, Y. Wang, S.M.K. Alam, and A. Nsabimana, Water Contamination and Human Health Risks in Pakistan: A Review, Exposure and Health 15 (2022) 619-639.

[9] S. Boulkhessaim, A. Gacem, S.H. Khan, A. Amari, V.K. Yadav, H.N. Harharah, A.M. Elkhaleefa, K.K. Yadav, S.U. Rather, H.J. Ahn, and B.H. Jeon, Emerging Trends in the Remediation of Persistent Organic Pollutants Using Nanomaterials and Related Processes: A Review, Nanomaterials (Basel) 12 (2022) 1-23.

[10] F. Elbehiry, T. Alshaal, N. Elhawat, and H. Elbasiouny, Environmental-friendly and cost-effective agricultural wastes for heavy metals and toxicants removal from wastewater, Cost-efficient Wastewater Treatment Technologies: Natural Systems, Springer, 2021, pp. 107-127.

[11] A. Sabitov, M. Atamanov, O. Doszhanov, K. Saurykova, K. Tazhu, A. Kerimkulova, A. Orazbayev, and Y. Doszhanov, Surface Characteristics of Activated Carbon Sorbents Obtained from Biomass for Cleaning Oil-Contaminated Soils, Molecules 29 (2024) 1-15.

[12] Z. Heidarinejad, M.H. Dehghani, M. Heidari, G. Javedan, I. Ali, and M. Sillanpää, Methods for preparation and activation of activated carbon: a review, Environ. Chem. Lett. 18 (2020) 393-415.

[13] D. Ouyang, X. Lei, and H. Zheng, Recent Advances in Biomass-Based Materials for Oil Spill Cleanup, Nanomaterials (Basel) 13 (2023) 1-37.

[14] M.M. Tijani, A. Aqsha, and N. Mahinpey, Development of oil-spill sorbent from straw biomass waste: Experiments and modeling studies, J. Environ. Manage. 171 (2016) 166-176.

[15] Y. Zhang, E.K. Sam, J. Liu, and X. Lv, Biomass-Based/Derived Value-Added Porous Absorbents for Oil/Water Separation, Wast. Biom. Valorization 14 (2023) 3147-3168.

[16] A.G. Adeniyi, C.A. Adeyanju, E.C. Emenike, S.K. Otoikhian, S. Ogunniyi, K.O. Iwuozor, and A.A. Raji, Thermal energy recovery and valorisation of *Delonix regia* stem for biochar production, Environ. Challenges 9 (2022) 1-33.

[17] E.C. Emenike, S. Ogunniyi, J.O. Ighalo, K.O. Iwuozor, H.K. Okoro, and A.G. Adeniyi, *Delonix regia* biochar potential in removing phenol from industrial wastewater, Biores. Tech, Reports 19 (2022).

[18] S. Azeez, I. Saheed, F. Adekola, A. Jimoh, D. Aransiola, and Z. Abdulsalam, Box Behnken Design in the Optimization of Rhodamine B Adsorption onto Activated Carbon Prepared from *Delonix regia* Seeds and Pods, J. Turk. Chem. Soc. Sec. A: Chemistry 9 (2022) 209-226.

[19] A.O. Ibrahim, A.O. Olagunju, S.O. Agboola, and O.S. Bello, Adsorption of amlodipine on surface-modified activated carbon derived from *Delonix regia* seed pod, J. Dispersion Sci. Technol. (2024) 1-13.

[20] G.K. Latinwo, A.O. Alade, S.E. Agarry, and E.O. Dada, Process Optimization and Modeling the Adsorption of Polycyclic Aromatic-Congo Red Dye onto *Delonix regia* Pod-Derived Activated Carbon, Polycyclic Aromat. Compd. 41 (2019) 400-418.

[21] A. Fisher, Sample Collection Methods, Atomic Spectrometric Methods of Analysis, Royal Society of Chemistry, 2025, 1, pp. 1-11.

[22] ASTM, "Standard Test Method for Total Oil and Grease (TOG) and Total Petroleum Hydrocarbons (TPH) in Water and Wastewater with Solvent Extraction using Mid-IR Laser Spectroscopy," ASTM International, 2022.

[23] ASTM, "Standard Practice for Proximate Analysis of Coal and Coke," ASTM International, 2013.

[24] ASTM, "Standard Test Method for Determination of Iodine Number of Activated Carbon," ASTM International, 2014.

[25] T.A. Afolabi, and D.G. Adekanmi, Characterization of Native and Graft Copolymerized Albizia Gums and Their Application as a Flocculant, J. Polym. 2017 (2017) 1-8.

[26] C. Ji, H. Yin, M. Zhou, Z. Sun, Y. Zhao, and L. Li, Adsorption of total petroleum hydrocarbon in groundwater by KOH-activated biochar loaded double surfactant-modified nZVI, Front. Mater. 10 (2023) 1-15.

[27] U. Anwana Abel, G. Rhoda Habor, and O. Innocent Oseribho, Adsorption Studies of Oil Spill Clean-up Using Coconut Coir Activated Carbon (CCAC), Am. J. Chem. Eng. 8 (2020) 1-12.

[28] P. Sugumaran, V.P. Susan, P. Ravichandran, and S. Seshadri, Production and characterization of activated carbon from banana empty fruit bunch and *Delonix regia* fruit pod, J. Sustain. Energy Environ. 3 (2012) 125-132.

[29] C. Bläker, J. Muthmann, C. Pasel, and D. Bathen, Characterization of Activated Carbon Adsorbents – State of the Art and Novel Approaches, ChemBioEng Rev. 6 (2019) 119-138.

[30] D. Bergna, T. Varila, H. Romar, and U. Lassi, Comparison of the Properties of Activated Carbons Produced in One-Stage and Two-Stage Processes, C 4 (2018) 41.

[31] O.I. Alonge, P.A. Oreoluwa, A.P. Okediji, O.A. Oloruntoba, and I.O. Alabi, "Characterization and Optimization of Carbonization of Flamboyant Tree Pod." pp. 1-8.

[32] G.K. Latinwo, A.O. Alade, S.E. Agarry, and E.O. Dada, Optimization of process parameters for the production of activated carbon from *Delonix regia* pod through chemical activation and carbonization process, Appl. J. Envir. Eng. Sci. 5 (2019) 75-98.

[33] Y. Fan, H. Wang, L. Deng, Y. Wang, D. Kang, C. Li, and H. Chen, Enhanced adsorption of Pb (II) by nitrogen and phosphorus co-doped biochar derived from Camellia oleifera shells, Environ. Res. 191 (2020) 110030.

[34] A. Eleryan, M. Hassaan, M.A. Nazir, S.S. Shah, S. Ragab, and A. El Nemr, Isothermal and kinetic screening of methyl red and methyl orange dyes adsorption from water by *Delonix regia* biochar-sulfur oxide (DRB-SO), Sci. Rep. 14 (2024) 1-16.

[35] D. Pattnaik, S. Kumar, S. Bhuyan, and S. Mishra, "Effect of carbonization temperatures on biochar formation of bamboo leaves." p. 012054.

[36] Y. Lee, J. Park, C. Ryu, K.S. Gang, W. Yang, Y.-K. Park, J. Jung, and S. Hyun, Comparison of biochar properties from biomass residues produced by slow pyrolysis at 500°C, Bioresour. Technol. 148 (2013) 196-201.

[37] A. Olowofoyeku, D. Adekanmi, and C. Ugwuanyi, Seasonal Variations and Correlation Analysis of Physicochemical Properties, Heavy Metals, and Petroleum-Derived Compounds in Borehole Water from Eneka and Alode Communities, Rivers State, Nigeria, J. Appl. Sci. Environ. Manage. 29 (2025) 1-11.

[38] D. Sivakumar, R. Parthiban, P.S. Kumar, and A. Saravanan, Synthesis and characterization of ultrasonic-assisted *Delonix regia* seeds: modelling and application in dye adsorption, Desalin. Water Treat. 173 (2020) 427-441.

[39] J. Utsev, R. Iwar, and K. Ifyalem, Adsorption of methylene blue from aqueous solution onto *Delonix regia* pod activated carbon: batch equilibrium isotherm, kinetic and thermodynamic studies, Agric. Wastes 4 (2020) 18-19.

[40] A. Esmaeili, and B. Saremnia, Comparison study of adsorption and nanofiltration methods for removal of total petroleum hydrocarbons from oil-field wastewater, J. Pet. Sci. Eng. 171 (2018) 403-413.

[41] J.C. Onwuka, E.B. Agbaji, V.O. Ajibola, and F.G. Okibe, Kinetic studies of surface modification of lignocellulosic *Delonix regia* pods as sorbent for crude oil spill in water, J. Appl. Res. Technol. 14 (2016) 415-424.

[42] M.K. Nazal, M. Ilyas, D. Gijjapu, and N. Abuzaid, Treatment of water contaminated with petroleum hydrocarbons using a biochar derived from seagrass biomass as low-cost adsorbent: isotherm, kinetics and reusability studies, Sep. Sci. Technol. 57 (2022) 2358-2373.